Communication

Site-Specific ^{13}C Chemical Shift Anisotropy Measurements in a Uniformly ^{15}N,^{13}C-Labeled Microcrystalline Protein by 3D Magic-Angle Spinning NMR Spectroscopy

Benjamin J. Wylie, W. Trent Franks, Daniel T. Graesser, and Chad M. Rienstra

J. Am. Chem. Soc., **2005**, 127 (34), 11946-11947• DOI: 10.1021/ja053862e • Publication Date (Web): 04 August 2005

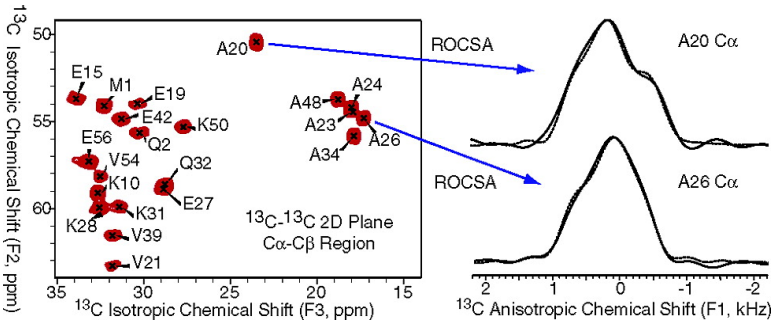

More About This Article

Additional resources and features associated with this article are available within the HTML version:

- Supporting Information
- Links to the 8 articles that cite this article, as of the time of this article download
- Access to high resolution figures
- Links to articles and content related to this article
- Copyright permission to reproduce figures and/or text from this article

View the Full Text HTML

J|A|C|S COMMUNICATIONS

Published on Web 08/04/2005

Site-Specific ^{13}C Chemical Shift Anisotropy Measurements in a Uniformly ^{15}N,^{13}C-Labeled Microcrystalline Protein by 3D Magic-Angle Spinning NMR Spectroscopy

Benjamin J. Wylie, W. Trent Franks, Daniel T. Graesser, and Chad M. Rienstra*

Department of Chemistry, University of Illinois at Urbana−Champaign, 600 South Mathews Avenue, Urbana, Illinois 61801

Received June 12, 2005; E-mail: rienstra@scs.uiuc.edu

The dependence of NMR isotropic chemical shifts on protein conformation can be utilized to constrain protein secondary structure in solution[1,2] and the solid state.[3] Quantum chemical calculations[4,5] and solution NMR measurements[6] reveal smaller Cα chemical shift anisotropy (CSA) magnitude in α-helical versus β-sheet conformations, and solid-state studies of small peptides have quantified the dependence of tensor parameters on backbone dihedral angles (ϕ,ψ).[4,7,8] The availability of theoretical shielding surfaces for all 20 common amino acids[5] motivates the development and application of CSA measurement techniques, such as recoupling sequences by Tycko et al. that enabled scaled, undistorted powder patterns to be site-resolved in 2D experiments.[9] Windowless sequences were developed to improve robustness with respect to frequency offsets and radio frequency (rf) inhomogeneity[10] in order to study U-^{13}C-labeled peptides.[11] Recently, Chang and Tycko utilized symmetry principles to devise the Recoupling of the Chemical Shift Anisotropy (ROCSA) sequence,[12] which suppresses homonuclear dipolar effects and reduces the rf field required, allowing application at >10 kHz MAS rates, where resolution in uniformly ^{13}C,^{15}N-labeled proteins is optimal.[13]

In this Communication, we report site-resolved CSA measurements in a microcrystalline protein of known structure (the 56 residue β1 immunoglobulin binding domain of protein G, GB1),[14] from a 3D experiment incorporating a ROCSA dimension (Figure 1). SPC-5 mixing,[15] soft-pulse decoupling of scalar $^{13}C-^{13}C$ couplings, and TPPM decoupling of the protons[16] yielded well-resolved and sensitive 3D spectra, from which 127 ROCSA line shapes were extracted, constituting 102 unique backbone and side-chain ^{13}C sites. The GB1 sample (~10 mg) was prepared as a microcrystalline precipitate in a 3.2 mm rotor as described elsewhere.[17] The ROCSA time domain signal was fit to simulations performed with SIMPSON,[18] to minimize the root-mean-squared deviation (RMSD) between experiment and simulation as a function of the tensor parameters and a phenomenological effective relaxation rate (see Supporting Information). Gly and Ala Cα line shapes (Figure 2) provided a basis for initial evaluation since both small peptide SSNMR studies[4,7,8] and solution NMR cross-correlation measurements[6] are available. In agreement with quantum chemical calculations[7] and previous solid-state measurements in ubiquitin,[19] our measurements showed smaller variations in the span ($\Omega = \delta_{11} - \delta_{33}$) between helix and sheet than typical for solution cross-correlation measurements.[6] This difference is ascribed to the relative orientation of the CSA to the Cα−Hα dipole vector.[4,19] As in the previous work of Hong,[19] the ROCSA technique allows for the direct comparison of experimental results to calculated chemical shielding surfaces.[4,5] The displayed "triple plot" (Figure 2b) illustrates the CSA tensor elements for the Cα resonances of the Gly and Ala residues of GB1, compared to calculations based upon the GB1 crystal structure of the T2Q mutant of GB1 (A. M. Gronenborn, unpublished). While there is little change in the span of these tensors, there are important overall shifts of the principal elements. G14, for example, resides in a turn, whereas G38 is positioned at the transition between the α-helix and the β3-strand; the downfield Cα isotropic shift of G38 arises primarily from a change in the δ_{11} tensor element. These results agree with the study of Wittebort et al. for Gly residues with similar secondary structure.[8]

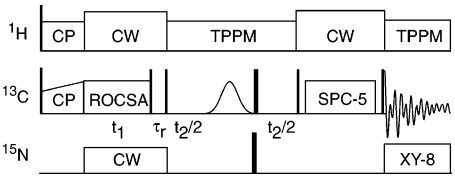

Figure 1. ROCSA−C−C 3D recoupling pulse sequence. ROCSA was applied under CW decoupling on ^{15}N and ^1H. A soft (Gaussian) pulse was placed in the middle of the t_2 evolution period to remove the influence of the scalar (CO−Cα and CO−Cβ) couplings. Narrow and wide rectangles represent $\pi/2$ and π pulses. Full experimental details, including phase cycles, are provided in the Supporting Information.

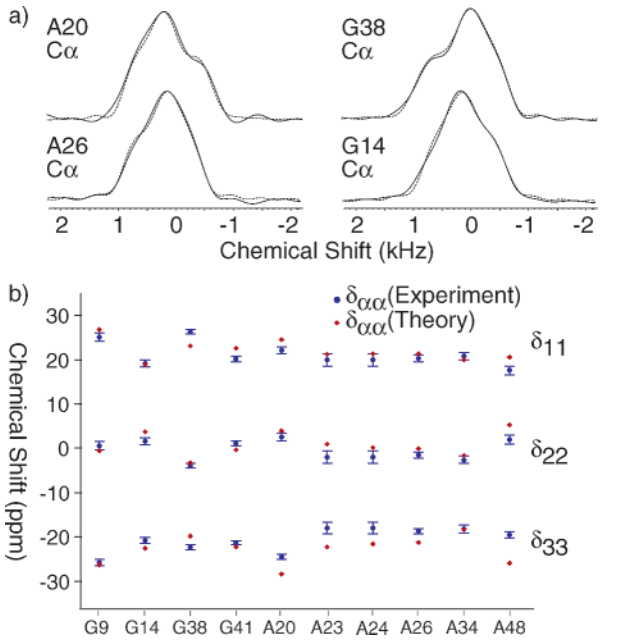

Figure 2. (a) ROCSA Cα powder patterns (solid line) with best-fit simulations (dotted). The label indicates the $^{13}C-^{13}C$ cross-peak from which CSA data were extracted. Data were sampled for 22 hypercomplex points with a dwell of 90 μs. (b) Plot of the principal components of Cα CSA tensor in the traceless representation for all Gly and Ala residues in GB1 (blue) compared to theoretical values assuming conformation from the crystal structure (red). Error bars were computed using a Monte Carlo algorithm as discussed in Supporting Information. The theoretical values shown here are not empirically scaled.

10.1021/ja053862e CCC: $30.25

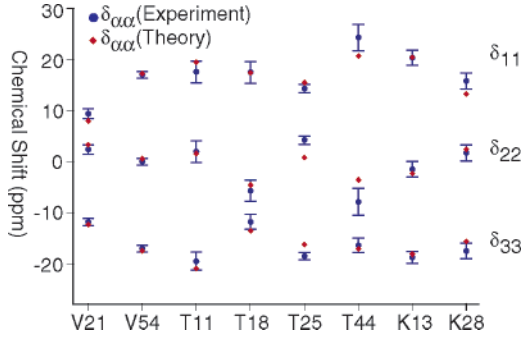

Figure 3. Plot of the principal components of the Cα CSA tensors (traceless) for selected Val, Lys, and Thr residues in GB1 (blue) versus theoretical values (red) based upon the crystal structure. Error bars were calculated using a Monte Carlo algorithm as discussed in Supporting Information. The theoretical values shown here are not empirically scaled.

A20, in a reverse β-turn, displays an upfield Cα isotropic shift due to δ_{33}, which shows a large variation relative to the helical Ala residues. Least-squares analysis of theory versus experiment shows a slope of -1.02 with a R^2 value of 0.99 for Gly, and a slope of -0.80 and a R^2 value of 0.98 for Ala. The RMSD between experiment and theory was 3.6 ppm for all Cα carbons studied here. When the theoretical values were scaled using the empirical factors reported by Havlin et al.,[4] the RMSD improved to 2.0 ppm.

Cα CSA tensors of Cβ-branched chain amino acids are especially sensitive to both backbone and side-chain conformation (χ_1).[4,5] For example, V21 (helical geometry) has a span of 21.2 ± 1.8 ppm, whereas V54 (in strand β4) has $\Omega = 35.1 \pm 1.5$ ppm. Thr Cα tensor elements demonstrate interesting conformational dependence, as the shielding surfaces exhibit multiple minima.[4,5] T11 Cα (in a near helical conformation) has a larger span (37.1 ± 3.9) than T18 (29.3 ± 3.6), which is located in strand β2; T25 (helical) has a span similar to that of T18 (32.0 ± 1.5), but with a *positive* δ_{22} (like T11). Both tensors are ~10 ppm narrower than T44 (41.0 ± 4.0), which is in the middle of a β-sheet. The relatively poor agreement with theory for T44 may be due to small changes in side-chain conformation, or that contributions from hydrogen bonding are not fully accounted for in the quantum chemical shielding surfaces. Differences as a function of conformation among long-chain residues, such as Lys, are less pronounced, but still much greater than the experimental error (e.g., between K13 (β-sheet) and K28 (α-helix)).

The precision of ROCSA for measuring smaller tensors also enables us to report (in the Supporting Information) values for 81 Cβ and other side-chain line shapes, reporting on 59 unique sites. For example, the Cβ tensor span of A20 is nearly twice as broad as those of the helical Ala residues, a more pronounced dependence upon (ϕ,ψ) conformation than the isotropic Cβ-shifts.[20] For Lys Cβ, large variations in the individual tensor elements arise despite similar secondary structures, demonstrating sensitivity to side-chain conformation and electrostatics. Thr Cβ line shapes vary substantially, and methyl ^{13}C tensors for Val, Ile, Met, and Thr vary in span from ~18 to more than 40 ppm and sample the full range of asymmetry, in a manner that depends little (if at all) upon backbone geometry.

In conclusion, we have introduced a 3D experiment to correlate CSA powder line shapes with isotropic chemical shifts, enabling 127 site-specific measurements in a protein. More efficient acquisition of CSA data will help to develop a database of experimental tensors from proteins of known structure to complement ongoing theoretical efforts for purposes of CSA-based structure refinement. CSA values measured directly in proteins will also aid in the design and interpretation of solution NMR experiments that utilize CSA−dipole cross-correlation, either to constrain torsion angles or to enhance resolution and sensitivity, such as in TROSY.[21]

Acknowledgment. The authors thank the University of Illinois, the American Chemical Society (Petroleum Research Fund), and the National Science Foundation (MCB 0347824) for funding, Prof. Eric Oldfield (University of Illinois) for discussions regarding chemical shifts, Dr. Angela Gronenborn (National Institutes of Health) for sharing the unpublished crystal structure of the GB1 T2Q mutant, and Dr. Paul Molitor (VOICE NMR Facility) for technical assistance.

Supporting Information Available: Details of data acquisition, processing and fitting procedures; examples of fitted line shapes; a table of measured tensor elements (PDF). This material is available free of charge via the Internet at http://pubs.acs.org.

References

(1) Spera, S.; Bax, A. *J. Am. Chem. Soc.* **1991**, *113*, 5490−5492.
(2) Wishart, D. S.; Sykes, B. D.; Richards, F. M. *J. Mol. Biol.* **1991**, *222*, 311−333.
(3) Luca, S.; Filippov, D. V.; van Boom, J. H.; Oschkinat, H.; de Groot, H. J. M.; Baldus, M. *J. Biomol. NMR* **2001**, *20*, 325−331.
(4) Havlin, R. H.; Laws, D. D.; Bitter, H. M. L.; Sanders, L. K.; Sun, H. H.; Grimley, J. S.; Wemmer, D. E.; Pines, A.; Oldfield, E. *J. Am. Chem. Soc.* **2001**, *123*, 10362−10369.
(5) Sun, H. H.; Sanders, L. K.; Oldfield, E. *J. Am. Chem. Soc.* **2002**, *124*, 5486−5495.
(6) Tjandra, N.; Bax, A. *J. Am. Chem. Soc.* **1997**, *119*, 9576−9577.
(7) Heller, J.; Laws, D. D.; Tomaselli, M.; King, D. S.; Wemmer, D. E.; Pines, A.; Havlin, R. H.; Oldfield, E. *J. Am. Chem. Soc.* **1997**, *119*, 7827−7831.
(8) Chekmenev, E. Y.; Xu, R. Z.; Mashuta, M. S.; Wittebort, R. J. *J. Am. Chem. Soc.* **2002**, *124*, 11894−11899.
(9) Tycko, R.; Dabbagh, G.; Mirau, P. A. *J. Magn. Reson.* **1989**, *85*, 265−274.
(10) Liu, S. F.; Mao, J. D.; Schmidt-Rohr, K. *J. Magn. Reson.* **2002**, *155*, 15−28.
(11) Hong, M.; Yao, X. L. *J. Magn. Reson.* **2003**, *160*, 114−119.
(12) Chan, J. C. C.; Tycko, R. *J. Chem. Phys.* **2003**, *118*, 8378−8389.
(13) McDermott, A.; Polenova, T.; Bockmann, A.; Zilm, K. W.; Paulsen, E. K.; Martin, R. W.; Montelione, G. T. *J. Biomol. NMR* **2000**, *16*, 209−219.
(14) Gallagher, T.; Alexander, P.; Bryan, P.; Gilliland, G. L. *Biochemistry* **1994**, *33*, 4721−4729.
(15) Hohwy, M.; Rienstra, C. M.; Jaroniec, C. P.; Griffin, R. G. *J. Chem. Phys.* **1999**, *110*, 7983−7992.
(16) Bennett, A. E.; Rienstra, C. M.; Auger, M.; Lakshmi, K. V.; Griffin, R. G. *J. Chem. Phys.* **1995**, *103*, 6951−6958.
(17) Franks, W. T.; Zhou, D. H.; Wylie, B. J.; Money, B. G.; Graesser, D. T.; Frericks, H. L.; Sahota, G.; Rienstra, C. M. *J. Am. Chem. Soc.* **2005**, in press.
(18) Bak, M.; Rasmussen, J. T.; Nielsen, N. C. *J. Magn. Reson.* **2000**, *147*, 296−330.
(19) Hong, M. *J. Am. Chem. Soc.* **2000**, *122*, 3762−3770.
(20) Saito, H.; Tabeta, R.; Sjohi, A.; Ozaki, T.; Ando, I. *Macromolecules* **1983**, *16*, 1050−1057.
(21) Pervushin, K.; Riek, R.; Wider, G.; Wuthrich, K. *Proc. Natl. Acad. Sci. U.S.A.* **1997**, *94*, 12366−12371.

JA053862E